Atomic and electronic properties of the Pb/Mo(110) adsorption system

K. Kośmider,[1,*] A. Krupski,[1] P. Jelínek,[2] and L. Jurczyszyn[1]
[1]*Institute of Experimental Physics, University of Wrocław, Pl. Maxa Borna 9, 50-204 Wrocław, Poland*
[2]*Institute of Physics, Department of Thin Films, Academy of Sciences of the Czech Republic, Cukrovarnicka 10, CZ-162 53 Praha 6, Czech Republic*
(Received 9 February 2009; published 18 September 2009)

We present the results of computational and experimental studies of the electronic and structural properties of the Pb/Mo(110) adsorption system. Computational part of this work is based on *ab initio* density-functional calculations. The obtained results provide detailed geometrical properties of different adsorption configurations and show the influence of lead coverage on the adsorption energy at different adsorption sites. We also consider the formation of ordered lead superstructures on the Mo(110) surface predicted by earlier experimental investigations as well as those indicated by our present scanning tunneling microscopy (STM) measurements. Our STM results show coexistence of two well-ordered surface superstructures in the first lead layer.

DOI: 10.1103/PhysRevB.80.115424 PACS number(s): 68.43.Bc, 68.37.Ef, 68.47.De, 71.15.Ap

I. INTRODUCTION

Information about the structural properties of fcc thin solid films located on bcc metal substrates is important for general understanding of the initial steps of growth of such deposition systems. Structural studies of the fcc/bcc systems provide a great deal of information on the connection between geometrical properties of the adsorbed layers and the atomic arrangement of the substrates. This knowledge might also be important in the context of controlled formation of surface nanostructures on bcc substrates.

The Pb/Mo(110) adsorption system was investigated two decades ago by Tikhov *et al.*[1] using low-energy electron diffraction (LEED), Auger electron spectroscopy (AES), and thermal-desorption spectroscopy. These measurements were limited to the temperature of about 350 K and allowed the authors to propose a set of models of ordered superstructures formed by lead on the Mo(110) surface. They found that all observed structures exhibit Pb adatoms arranged in rows parallel to the most closely packed substrate direction. This experimental study indicated also that the adsorption energy of Pb adatoms increases with increasing coverage. Later, the same system was investigated by reflection high-energy electron diffraction (RHEED) and scanning electron microscopy by Jo *et al.*[2] They proposed several distinct Pb surface superstructures arise on Mo(110).

Recently, Krupski[3] used scanning tunneling microscopy (STM) to study the growth of thin Pb films on the Mo(110) surface at room temperature (RT). The analysis of their STM results indicates that for coverages of $\theta<1$ ML, a two-dimensional growth of the first Pb monolayer takes place. Since, our present work is just related to such small coverages, we do not consider here the growth of three-dimensional structures. Nevertheless, to draw a wider context of this problem, it is worth to mention peculiar behavior of the Pb/Mo(110) system for greater coverages. In the layer-plus-island growth, lead islands showed strongly preferred atomic scale heights and flat tops.[3] At coverages between $1<\theta<2$ ML, only islands containing two atomic layers of Pb have been observed. At higher coverages $\theta>3$ ML, island height distribution shows strong peaks corresponding to 2, 4, 6, and 9 Pb atomic layers. Similar peculiar behavior of Pb adlayers has been observed on the Si(111) surface (see, e.g., Refs. 4–6) and the origin of this effect is still a subject of lively discussion. From this point of view, a detailed study of the corresponding system with metallic substrate can help understand the behavior of Pb adlayers, in general.

The analysis of various aspects of the growth of lead on a metallic substrate such as Mo(110) requires deeper understanding of physical properties of the Pb/Mo(110) system. So far, however, there is a lack of any theoretical studies related to the adsorption of lead on Mo(110). Therefore, in the present study we focus on the description of the response of the Mo(110) substrate to lead adatoms. The aim of the first step of this study is to determine the energetic order of different stable atomic configurations of Pb/Mo(110), analyze their structural and electronic properties, and clarify how the changes of coverage influence the adsorption energy of a lead adatom at different surface sites. To this end, we simulate adsorption process for different adsorption points and three different coverages, namely, 0.125, 0.25, and 0.5 ML. The obtained information enables us to perform further studies related to the formation of ordered superstructures found in experiment. On the basis of results obtained in the first stage, we propose structural models of surface superstructures indicated by experimental data. We perform structural relaxations of the proposed models, which enables us to check their stability and determine the details associated with their geometrical and energetic properties. The obtained results are analyzed and discussed in the context of experimental data.

II. METHOD OF CALCULATION

Theoretical study presented in this paper has been performed using *ab initio* calculations based on the density-functional theory and plane-wave basis set, as implemented in VASP package.[7–9] The electron-ion interactions have been described by the projector augmented wave method,[10] whereas the exchange-correlation contributions have been evaluated in the PW91 formulation[11] of the generalized gradient approximation (GGA). However, some checking calcu-

TABLE I. Selected parameters of the clean Mo(110) surface: $\Delta d_{i,j}$ are relaxation factors (relative changes in interlayer distances with respect to the bulk value d_0), σ is the surface energy while W is the work function.

	Number of layers	$\Delta d_{1,2}$ ($\%d_0$)	$\Delta d_{2,3}$ ($\%d_0$)	$\Delta d_{3,4}$ ($\%d_0$)	σ (J/m^2)	W (eV)
LDA	7	−5.42	0.49	0.00	3.16	4.89
	9	−5.14	0.72	0.11	3.36	4.87
GGA	7	−5.64	0.72	−0.02	2.60	4.60
	9	−5.38	0.91	0.14	2.75	4.59
	13	−5.40	0.87	0.10	2.77	4.61
LDA[a]	7	−4.5	0.5	0.0		
LDA[a]	9	−5.0	0.7	−0.3		
LDA[b]	7	−3.9			3.14	4.94
LEED[c]		−4.0	2.0	0.0		

[a]Reference 15.
[b]Reference 16.
[c]Reference 12.

lations have also been performed using the local-density approximation (LDA). The Davison-block algorithm has been used for electronic energy minimization while the conjugate gradient method has been employed to relax atomic positions. In all calculations, the plane-wave basis set has been determined by the energy cutoff of 300 eV. In the relaxed structures, the forces acting on particular atoms have been smaller than 0.003 eV/Å. We point out that all calculations presented in this paper have been performed without spin-orbit coupling.

The energy minimization of the bulk unit cell yields the Mo lattice parameter equal to 3.11/3.15 Å for LDA/GGA. Taking into account the corresponding experimental result of 3.15 Å provided by LEED measurements,[12] and the general tendency of LDA to underestimate the lattice constant, we conclude a good agreement between the calculated value and the experimental data. The bulk modulus has been evaluated within the Murnaghan equation of state. The calculated values of 2.70 Mbar for GGA and 3.01 Mbar for LDA are close to the experimental one of 2.73 Mbar.[13]

III. EXPERIMENT

The measurements have been carried out in a metal ultrahigh-vacuum chamber with the base pressure of 2×10^{-10} mbar. The chamber has been equipped with reverse-view LEED optics, AES, and the Omicron I variable-temperature STM. The Mo(110) crystal has been mounted on a home-built transferable sample holder with an integrated electron-beam heater. The sample could be heated up to 2400 K. The crystal temperature has been measured using the W5%Re–W26%Re thermocouple. The Mo(110) crystal has been cleaned by repeated flashing (30×5 min) at 1200 K in $p=3 \times 10^{-7}$ mbar oxygen atmosphere to remove the residual carbon contamination. Next, oxygen has been removed by flashing the sample at 2400 K for 15 s. Flashing at 2400 K has been repeated before each experiment. This procedure has been continued until the carbon peak in AES spectrum became invisible and a LEED pattern of the clean Mo(110) face with sharp spots and low background has been obtained. Lead (99.999%) has been evaporated onto the crystal surface from a quartz crucible surrounded by a tungsten resistive heater. The chamber pressure during evaporation has been kept below $p=3 \times 10^{-10}$ mbar. The STM images have been observed at RT. Tungsten STM tips have been used and the STM data have been processed using a freeware image-processing software.[14]

IV. RESULTS AND DISCUSSION

A. Clean Mo(110) substrate

In the first step of our theoretical study, we have considered the atomic and electronic properties of a clean Mo(110) substrate. Calculation of the Mo(110) surface have been performed by symmetrical relaxation of slab composed of an odd number of atomic layers (from 7 to 13) with two atoms per layer. In each case, the subsequent slabs have been separated by the vacuum region at least 8.5 Å thin. The surface Brillouin zone has been sampled by $(9 \times 9 \times 1)$ Monkhorst-Pack grid, which yields 36 irreducible special **k** points.

The obtained results indicate that the relaxation process of the Mo(110) surface system is limited solely to its topmost part (cf. Table I). The first interlayer distance $d_{1,2}$ is reduced by 5% (i.e., somewhat above 0.1 Å) while the subsequent distance $d_{2,3}$ is increased by 0.5–0.9 % (0.01–0.03 Å). The changes in the third interlayer distance $d_{3,4}$ are already negligibly small. These results are in good agreement with earlier theoretical studies[15–18] as well as LEED measurements.[12] The results presented in Table I show that the increase in the slab thickness above seven layers does not change considerably the atomic structure of the surface. Therefore, in the rest part of this work the Mo(110) surface has been described by a slab composed of seven atomic layers.

Figure 1 presents local density-of-states (LDOS) distributions calculated for the three topmost atomic layers of Mo(110). The obtained results indicate that electronic states in the energy range around the Fermi level are distinctly

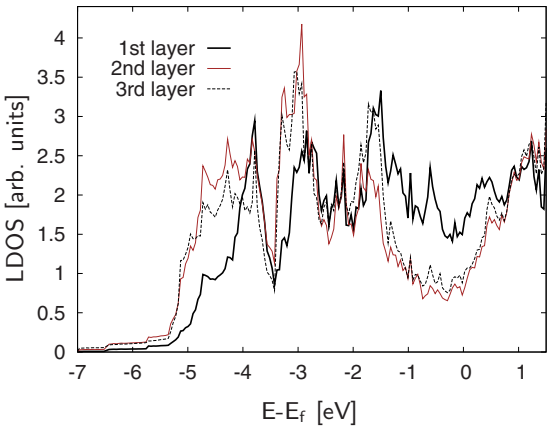

FIG. 1. (Color online) LDOS at the first (black, solid), second (brown, solid), and third (black, dashed) layer of a clean Mo(110) surface. Each curve represents a sum over all atoms within particular layer.

localized at the surface atomic layer while for lower energies their localization is shifted toward subsurface layers. LDOS distribution calculated for the topmost atomic layer shows that the surface electronic structure of Mo(110) is dominated by *d* states within the whole considered energy range (cf. Fig. 2).

B. Pb adsorption on the Mo(110) surface

In this section, we analyze the energetic, structural, and electronic properties of the Pb/Mo(110) system. In this study, the substrate has been represented by an asymmetric slab (composed of seven atomic layers). Atoms from the top four layers have been allowed to relax while the remaining part of the slab has been kept frozen with atoms fixed in their bulk-like positions. Adsorption of Pb has been simulated only on the relaxed side of the slab (with dipole-moment corrections applied). We have checked that such a substrate reproduces correctly the structural and electronic properties of the clean Mo(110) surface described in previous section.

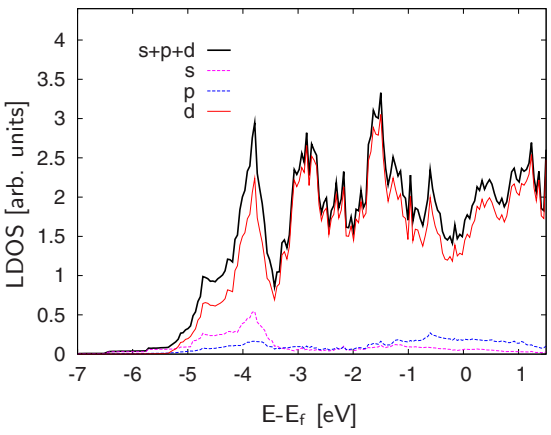

FIG. 2. (Color online) LDOS of the topmost Mo(110) layer (black, solid) and its components associated with *s* (pink, dashed), *p* (blue, dashed), and *d* (red, solid) orbitals (cf. Fig. 1).

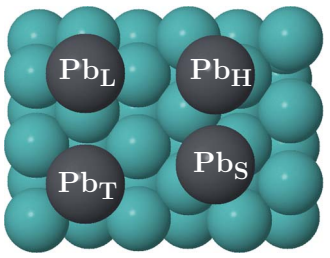

FIG. 3. (Color online) Considered points of Pb adsorption on the Mo(110) surface.

Simulations of the adsorption of Pb atoms have been performed for four different adsorption sites schematically shown in Fig. 3. In order to analyze the interaction of Mo(110) substrate with Pb adatoms, we first considered a rather low coverage of 0.125 ML, which simulates adsorption of quasi-isolated Pb adatoms (interaction between adatoms is negligible). Results of structural calculations indicate that configurations L, S, and T are stable, while Pb atom originally placed at site H moves toward position L. To determine the energetic relations between different stable configurations, we have calculated the adsorption energy E_b defined as

$$E_b = -\frac{1}{N}(E_{\mathrm{Pb/Mo(110)}} - E_{\mathrm{Mo(110)}} - NE_{\mathrm{Pb}}), \qquad (1)$$

where $E_{\mathrm{Mo(110)}}$ is the energy of a clean Mo(110) slab, $E_{\mathrm{Pb/Mo(110)}}$ is the energy of an adsorbed slab, and E_{Pb} is the energy of a free Pb atom while N is the number of adsorbate atoms in the cell.

For the coverage of 0.125 ML, the adsorption energy E_b(L) at point L is 0.25 and 0.61 eV larger than E_b(S) and E_b(T), respectively (cf. Table II). For greater coverages (θ =0.25 and θ=0.5), we have found the same energetic order of adsorption points [i.e., E_b(T)$<E_b$(S)$<E_b$(L)]

Geometry of the relaxed Pb/Mo(110) system indicates that adsorption of Pb adatoms modifies considerably the position of substrate atoms, shifting them vertically and laterally with respect to the clean Mo(110) structure. For a low coverage of 0.25 ML, structural changes in the Mo(110) substrate have a rather complex character. This is illustrated in Fig. 4, which sketches the response of the Mo(110) substrate to the adsorption of Pb adatoms at lattice point L. The shift of particular Mo atoms varies from around 0.1 Å (for the topmost atoms) to around 0.01 Å (for atoms in the fourth layer). For a higher coverage of 0.5 ML, the substrate re-

TABLE II. Adsorption energies calculated from Eq. (1).

θ (ML)	E_b (eV)		
	L	S	T
0.125	4.49	4.23	3.88
0.250	4.39	4.13	3.85
0.500	4.41	4.22	4.00

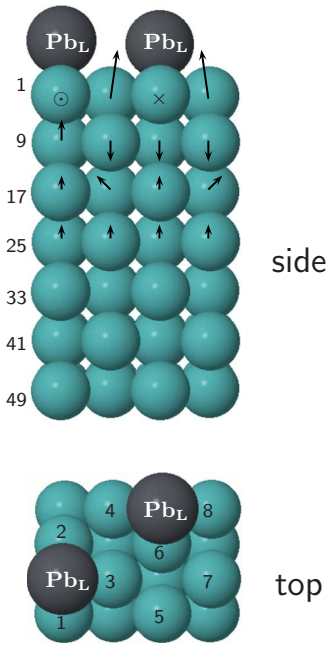

FIG. 4. (Color online) Atomic arrangement of the supercell used for simulations of adsorption of 0.25 ML of Pb at points L of the Mo(110) surface. Arrows indicate a response of the Mo(110) substrate to the presence of Pb adatom.

sponses in a more systematic way, as shown in Fig. 5. Pb adatoms located at points L or T change only vertical coordinates of the substrate atoms (cf. Table III), while for point S the horizontal coordinates are also modified (symmetrically). Table IV presents the final Pb distance to the topmost-layer Mo atoms for points L, S, and T.

LDOS distributions shown in Fig. 6 represent the electronic structure of the Pb/Mo(110) system for the coverage of 0.5 ML. The obtained dependences indicate that the presence of Pb atoms leads to visible changes in the surface electronic structure. The presence of the Pb atoms introduces a set of LDOS features in the energy range from −10 up to −7 eV and slightly enhances the total LDOS for energies between −3 and 2 eV (cf. Fig. 6). Moreover, Fig. 7 shows that these are just the energy ranges where the contribution from Pb adatoms to the total surface DOS is significant.

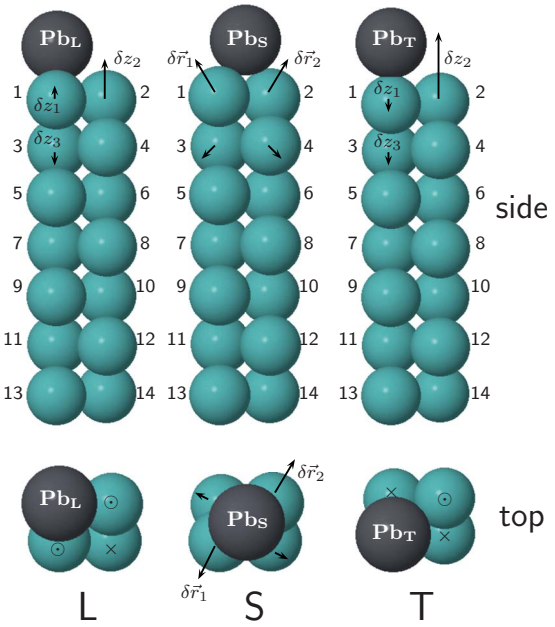

FIG. 5. (Color online) The same as in Fig. 4 but for adsorption points L, S, and T, and the coverage of 0.5 ML.

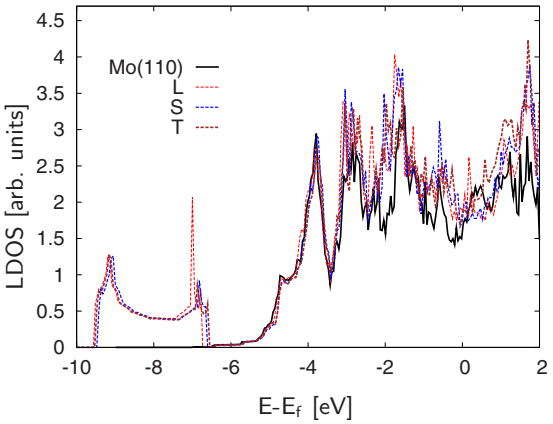

FIG. 6. (Color online) LDOS distributions for the Pb/Mo(110) system (the sum of LDOS contributions associated with Pb adatom and two surface Mo atoms) in configuration L (red, dashed), S (blue, dashed), and T (brown, dashed), compared with the LDOS distribution for a clean Mo(110) surface (black, solid; cf. Fig. 2). Coverage θ=0.5 ML.

C. Pb structures on the Mo(110) surface

Experimental data provided by LEED at T=350 K,[1] RHEED at T between 300 and 1100 K,[2] and also by our present STM measurements at T=300 K (see below) indicate that Pb atoms adsorbed on the Mo(110) substrate form a number of ordered superstructures with different geometrical properties. In this section we analyze a few selected superstructures identified by these measurements.

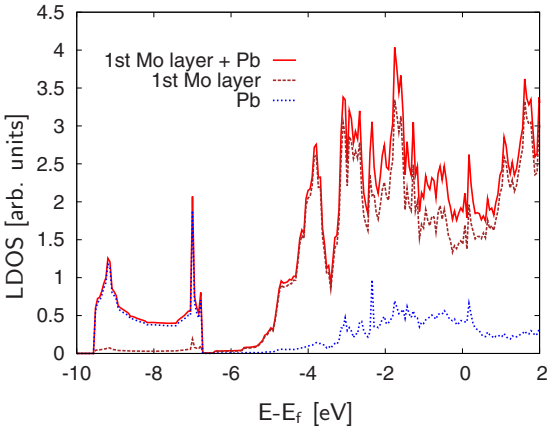

FIG. 7. (Color online) LDOS for configuration L of the Pb/Mo(110) system and coverage of 0.5 ML (red, solid; cf. Fig. 6) and its components connected with the surface Mo layer (brown, dashed) the adsorbed Pb$_L$ atom (blue, dashed).

TABLE III. Changes in the Mo(110) surface geometry induced adsorption of 0.5 ML of Pb (see slab structure in Fig. 5). All values are in Å.

		First Mo layer					
		$\delta\vec{r}_1$			$\delta\vec{r}_2$		
		δx_1	δy_1	δz_1	δx_2	δy_2	δz_2
S	GGA	−0.03	−0.06	0.06	0.03	0.06	0.06
	LDA	−0.03	−0.05	0.06	0.03	0.05	0.06
		First Mo layer		Second Mo layer			
		δz_1		δz_2	δz_3		δz_4
T	GGA	−0.02		0.15	−0.03		0.00
	LDA	−0.03		0.15	−0.03		0.00
L	GGA	0.03		0.09	−0.03		0.00
	LDA	0.03		0.09	−0.03		0.00

On the basis of results of LEED measurements performed for the Pb/Mo(110) system with the coverage of 2/3 ML, Tikhov *et al.*[1] proposed two Pb superstructures, as shown in Fig. 8. Both configurations differ from each other in the position of half of the Pb atoms. In case (a), the superstructure is composed of Pb atoms placed in adsorption sites L and S (atoms Pb_L and Pb_S, respectively), whereas in case (b), Pb adatoms are located in points L and H (adatoms Pb_{L_1}, Pb_{L_2}, and Pb_H). To check the stability of these structures and to determine their geometrical and energetic properties, we have performed their structural relaxation. In configuration (a), relaxation does not introduce any lateral shifts of Pb adatoms but Pb_S atoms protrude 0.11 Å above Pb_L ones. In structure (b), like for the case of lower coverages (cf. Sec. IV B), relaxation modifies the lateral position of Pb_H atoms (located initially at point H), decreasing their distance to Pb_{L_2} atoms by about 0.16 Å (positions of Pb_{L_1} and Pb_{L_2} atoms remain fixed). Consequently, after relaxation, the distance of Pb_H atoms to the closest Pb_{L_1} and Pb_{L_2} atoms equals to 3.51 and 3.55 Å, respectively. Moreover, Pb_H atoms are located 0.02 Å above Pb_{L_1} and 0.14 Å above Pb_{L_2} ones. Superstructures (a) and (b) are represented by the same translational symmetry and consequently, the same unit cell has been used (see Fig. 8). Comparison of their total energies indicate that structure (b) is energetically more favorable, which is consistent with the predictions presented in Ref. 1. We have also calculated the average adsorption energy (i.e., E_b averaged over four adatoms within the unit cell; note that each superstructure is composed of different adsorption sites, cf. Fig. 8) and obtained 4.41 and 4.43 eV for superstructures (a) and (b), respectively. Hence, the energetic properties of both systems are close to each other.

In our present work, the formation of ordered surface structures in the Pb/Mo(110) adsorption system has also been investigated experimentally using STM. Experimental data have been obtained after deposition of lead on the Mo(110) surface at RT (cf. Fig. 9). Closer view of the STM image topography in Fig. 10 reveals the presence of two well-ordered lead superstructures denoted ϵ_1 and ϵ_2. Their geometrical parameters are described in the caption of Fig. 10. The structures ϵ_1 and ϵ_2 have been observed simultaneously at different parts of the Mo(110) substrate. STM images indicate in both cases a long-range order in the surface system. The density of Pb atoms determined for the ϵ_1 and ϵ_2 structures is 4.5×10^{14} and 6.4×10^{14} atoms/cm^2, respectively, which is 48% and 68% of the density of the close-packed (111) Pb layer (equal to 9.4×10^{14} atoms/cm^2).

Taking into account our experimental results, we have considered structural models of the Pb/Mo(110) surface reproducing best the topography of the obtained STM images. The model of ϵ_1 assumes that the superstructure is built up by Pb_L and Pb_S adatoms with the coverage of 1/3 ML (cf. Fig. 11). The lateral geometrical properties of this model (distances between the nearest lead adatoms along the directions $\vec{a}$ and $\vec{b}$ and the angle between them) are almost the same as those following STM measurements (cf. captions of Figs. 10 and 11). Structural relaxation have shown that such a model is stable, i.e., the lateral positions of all lead adatoms in the relaxed structure are the same as in the starting con-

TABLE IV. Distances between the Pb adatom (0) and topmost-layer Mo atoms (1 and 2, in accordance with notation used in Fig. 5). All values are in Å. Coverage θ=0.5 ML.

	L		S	T	
	d_{01}	d_{02}	$d_{01}=d_{02}$	d_{01}	d_{02}
LDA	2.90	3.24	2.86	2.71	3.70
GGA	2.96	3.31	2.93	2.78	3.78

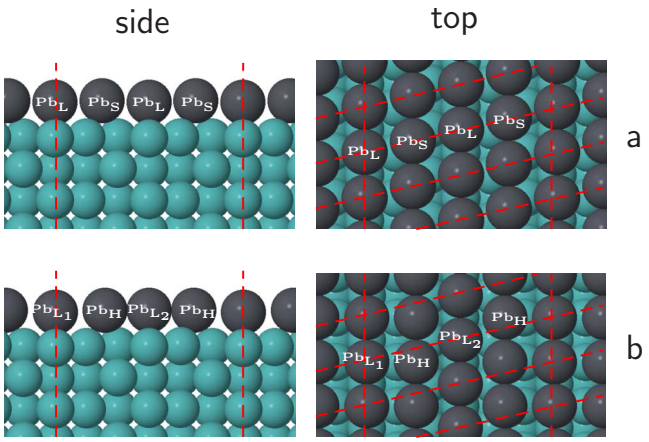

FIG. 8. (Color online) Geometrical model of the Pb/Mo(110) superstructure with coverage $\theta=2/3$ ML observed by Tikhov *et al.*(Ref. 1): (a) structure consisting of L and S adsorption points and (b) structure consisting of L and H adsorption points (cf. Fig. 3). Red dashed lines denote the supercells used in simulations.

figuration while Pb_S adatoms protrude 0.08 Å above Pb_L. The superstructure ϵ_2 is, in turn, modeled by an adlayer with Pb_L, Pb_S, and Pb_T atoms (cf. Fig. 12), corresponding to the coverage of 4/9 ML. The lateral parameters of this model (i.e., a, b, and α) reproduce well the STM data (cf. captions of Figs. 10 and 12). Results of structural simulations show that Pb_T adatoms are located 0.09 Å above Pb_S and 0.17 Å above Pb_L while the lateral positions of all lead atoms remain fixed during the relaxation. The supercells used for simulations of both superstructures are different, so a direct comparison of their total energies is not possible. Thus, to determine the energy relationship between them, we have calculated the average adsorption energy per one Pb adatom. To this end, E_b was averaged over two or four adatoms from the supercell corresponding to the superstructure ϵ_1 and ϵ_2, respectively (cf. Figs. 11 and 12). Such obtained averaged adsorption energy equals to 4.28 eV for ϵ_1 and 4.29 for ϵ_2.

We would like to point out that energetic properties of the lead superstructures considered in this section are consistent

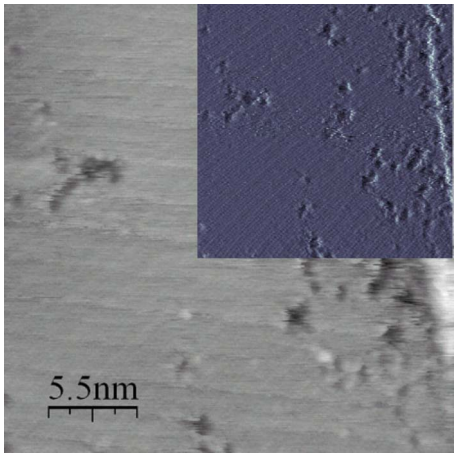

FIG. 9. (Color online) STM image (275 Å×275 Å) of Pb adsorbed on Mo(110): $T=300$ K, $U_{bias}=149$ mV, $I_T=1.7$ nA. Inset present differentiated STM image with enhanced contrast.

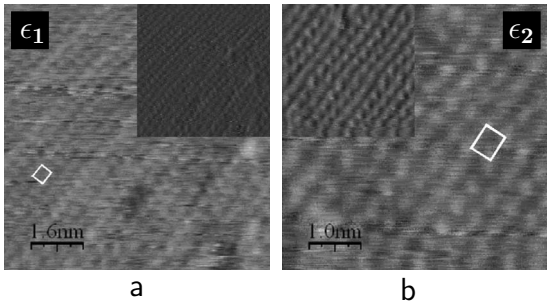

FIG. 10. STM images (differentiated in insets) of two kinds of Pb superstructures (ϵ_1 and ϵ_2) observed on Mo(110): (a) image size 80 Å×80 Å, $T=300$ K, $U_{bias}=149$ mV, $I_T=1.7$ nA; (b) image size 50 Å×50 Å, $T=300$ K, $U_{bias}=76$ mV, $I_T=3.3$ nA. White parallelograms indicate unit cells of the respective Pb structures with geometrical parameters measured to be equal to $a=4.3$ Å, $b=5.2$ Å, and $\alpha=84°$ for ϵ_1, and $a=4.1$ Å, $b=3.8$ Å, and $\alpha=92°$ for ϵ_2 (cf. Figs. 11 and 12).

with experimental results presented in Ref. 1, indicating that adsorption energy of lead adatoms increases with coverage. Indeed, adsorption energies calculated for dense superstructures shown in Fig. 8 (corresponding to the coverage of 2/3 ML) are above 4.4 eV, which is noticeably higher than the values (below 4.3 eV) obtained for more dilute superstructures given in Figs. 11 and 12.

V. SUMMARY

We have presented computational and experimental studies of the atomic and electronic properties of the Pb/Mo(110) adsorption system. Structural relaxation of the clean Mo(110) surface system indicates that significant changes in interlayer distances are limited to three topmost layers only, which corresponds well to the results of earlier theoretical and experimental studies.

First, we have simulated adsorption of quasi-isolated Pb atom on Mo(111) by considering the coverage $\theta=0.125$ ML. We have found the following energetic preferences of the adsorbate with respect to possible adsorption

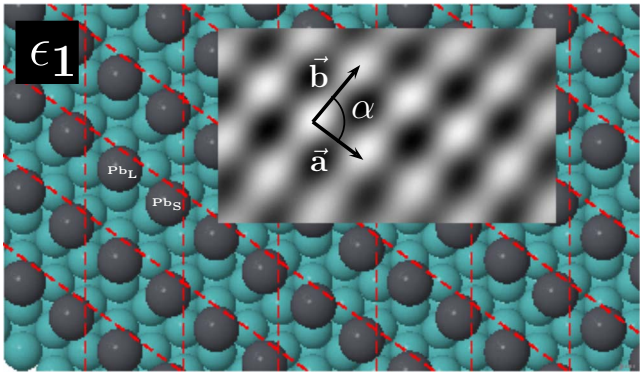

FIG. 11. (Color online) Overlap of the geometrical model of the superstructure ϵ_1 with its filtered STM image. Parameters of the simulated unit cell are $a=4.1$ Å, $b=5.2$ Å, and $\alpha=84°$ [cf. Fig. 10(a)]. Red dashed lines denote the supercells used in simulations.

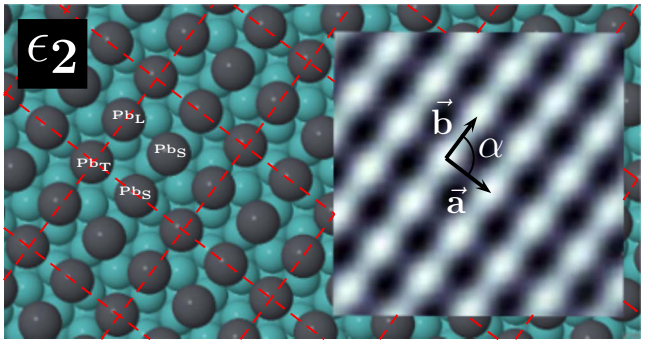

FIG. 12. (Color online) The same as in Fig. 11 but for the superstructure ϵ_2. Parameters of the simulated unit cell are: a =4.1 Å, b=3.9 Å, and α=90° [cf. Fig. 10(b)].

points: $E_b(\mathrm{T}) < E_b(\mathrm{S}) < E_b(\mathrm{L})$ (point H is not stable). Those preferences are maintained for higher coverages of 0.25 and 0.5 ML.

In accordance with earlier experimental LEED data and our present STM measurements, we have considered the formation of selected ordered Pb superstructures in the Pb/Mo(110) system. Structural calculations have been performed for two dense Pb superstructures (corresponding to θ=2/3 ML) found previously by Tikhov *et al.*[1] The obtained results confirm the energetic order predicted for these two systems and allowed us to determine the details of their atomic geometry. We have found that the surface corrugation of both superstructures is within 0.1 Å.

Our present RT STM observations indicate the coexistence of two kinds of Pb superstructures (ϵ_1 and ϵ_2) exhibiting a long-range order. These results complement other experimental data on lead superstructures obtained in RT conditions.[2] Taking into account the properties of the Pb/Mo(110) system determined in the first part of our study, we have proposed geometrical models of both superstructures. Their structural parameters (i.e., the lattice vectors and the angle between them) are very close to those measured experimentally. The coverages derived from these models equal to 1/3 and 4/9 ML for ϵ_1 and ϵ_2, respectively. Relaxation performed for both systems indicates that their surface corrugation is within 0.08 Å for ϵ_1 and 0.17 Å for ϵ_2. The average adsorption energies of superstructures ϵ_1 and ϵ_2 are about 0.1 eV lower than those of the denser Tikhov's superstructures. This confirms the tendency of E_b to be higher for denser superstructures, in accordance with Ref. 1.

ACKNOWLEDGMENTS

The work of P.J. has been supported by the GACR grant No. 202/09/0775 and the GAAV grants No. IAA100100905, No. IAA100100616, and No. AV0Z10100521. Numerical calculations reported in this work have been performed at the Interdisciplinary Centre for Mathematical and Computational Modeling of the University of Warsaw within the Grant No. G31–20.

*Corresponding author; kko@ifd.uni.wroc.pl

[1] M. Tikhov and E. Bauer, Surf. Sci. **203**, 423 (1988).
[2] S. Jo, Y. Gotoh, T. Nishi, D. Mori, and T. Gonda, Surf. Sci. **454-456**, 729 (2000).
[3] A. Krupski, Phys. Rev. B **80**, 035424 (2009).
[4] H. Hong, C.-M. Wei, M. Y. Chou, Z. Wu, L. Basile, H. Chen, M. Holt, and T.-C. Chiang, Phys. Rev. Lett. **90**, 076104 (2003).
[5] Z. Kuntova, M. Hupalo, Z. Chvoj, and M. Tringides, Surf. Sci. **600**, 4765 (2006).
[6] W. B. Jian, W. B. Su, C. S. Chang, and T. T. Tsong, Phys. Rev. Lett. **90**, 196603 (2003).
[7] G. Kresse and J. Hafner, Phys. Rev. B **47**, 558 (1993).
[8] G. Kresse and J. Furthmüller, Comput. Mater. Sci. **6**, 15 (1996).
[9] G. Kresse and J. Furthmüller, Phys. Rev. B **54**, 11169 (1996).
[10] G. Kresse and D. Joubert, Phys. Rev. B **59**, 1758 (1999).
[11] J. P. Perdew and Y. Wang, Phys. Rev. B **45**, 13244 (1992).
[12] M. Arnold, S. Sologub, G. Hupfauer, P. Bayer, W. Frie, L. Hammer, and K. Heinz, Surf. Rev. Lett. **4**, 1291 (1997).
[13] K. A. Gschneidner, in *Advances in Research and Applications*, Solid State Physics Vol. 16, edited by F. Seitz and D. Turnbull (Academic, New York, 1964), pp. 275–426.
[14] Nanotec, http://www.nanotec.es, 2009.
[15] B. Kohler, P. Ruggerone, and M. Scheffler, Phys. Rev. B **56**, 13503 (1997).
[16] M. Methfessel, D. Hennig, and M. Scheffler, Phys. Rev. B **46**, 4816 (1992).
[17] J. G. Che, C. T. Chan, W.-E. Jian, and T. C. Leung, Phys. Rev. B **57**, 1875 (1998).
[18] B. Kohler, P. Ruggerone, S. Wilke, and M. Scheffler, Phys. Rev. Lett. **74**, 1387 (1995).